Current Trends in Endocrinology
Vol. 7, 2014

Original Communication

Role of T-type Ca^{2+} channels in basal $[Ca^{2+}]_i$ regulation and basal insulin secretion in rat islet cells

Brian M. Keyser[1], James T. Taylor[2], Soo-Kyoung[3], Yujie Lu[4], Arin Bhattacharjee[5], Luping Huang[3], Jonathan Pottle[3], Khalid Matrougui[3], Zihui Xu[4,#] and Ming Li[3,*,#]

[1]Cell and Molecular Biology Branch, Research Division, US Army Medical Research Institute of Chemical Defense, [2]Operational Toxicology, Science Applications International, Edgewood Chemical Biological Center, Aberdeen Proving Ground, MD 21010, USA, [3]Department of Physiology, Tulane University Health Sciences Center, New Orleans, LA 70112, USA. [4]Department of Integrative Medicine, Xinqiao Hospital, Third Military Medical University, Chongqing, 400037, China. [5]Department of Pharmacology and Toxicology, The State University of New York at Buffalo, Buffalo, NY 14214, USA

ABSTRACT

Elevated level of basal insulin secretion is a characteristic of type 2 diabetes mellitus. The mechanism underlying the phenomenon is poorly understood. We found T-type Ca^{2+} channel window currents contributive to increased basal $[Ca^{2+}]_i$ in β-cells. Rat islet cells incubated in 11.1 mM glucose were found to have up-regulated $Ca_v3.1/3.2$ mRNA and protein expression and elevated basal $[Ca^{2+}]_i$. The increase in basal $[Ca^{2+}]_i$ was substantially decreased in the presence of NNC 55-0396 and siRNA targeting $Ca_v3.1$ and $Ca_v3.2$. High glucose exposure also contributed to elevated basal insulin secretion, which was reduced by chelating intracellular calcium or calcium antagonists. An *in vivo* study showed that T-type Ca^{2+} channel antagonists greatly reduced stable levels of insulin in a diabetic rodent model.

*Corresponding author: Dr. Ming Li, Ph.D.
SL-39, 1430 Tulane Avenue, New Orleans,
LA 70112, USA.
mli@tulane.edu

[#]Z. Xu and M. Li contributed equally to this work and should be considered as corresponding authors.

KEYWORDS: T-type Ca^{2+} channels, NNC 55-0396, $Ca_v3.1$, $Ca_v3.2$, diabetes, intracellular calcium, electrophysiology

INTRODUCTION

Clinical studies have shown that many people who develop type 2 diabetes mellitus not only have persistently elevated blood glucose but also have elevated basal insulin levels, years to decades before onset of the disease [1, 2]. Another phenomenon commonly associated with the disease is elevated basal intracellular calcium ($[Ca^{2+}]_i$) in a large number of cell types including pancreatic β-cells [3-5]. This elevation in $[Ca^{2+}]_i$ in β-cells has been found to be linked to a reduction in insulin release in response to a stimulation by glucose [5]. However, the role of β-cell basal level of calcium in controlling basal insulin release has not been studied.

Reduced insulin sensitivity has been correlated with elevated basal insulin levels [6]; however, the exact mechanisms that regulate basal insulin release remain unclear. It is generally accepted that glucose stimulated insulin release requires a large sustained membrane depolarization; basal insulin release is believed to occur via a different mechanism. Since membrane-localized increases

in calcium have been shown to trigger vesicular release of insulin [7, 8] and T-type Ca^{2+} channels have been found to mediate transient calcium influx in β-cells without a substantial membrane depolarization [9, 10], it is possible that these channels are responsible, at least in part, for regulating basal insulin release. To date there have been three T-type Ca^{2+} channel genes identified, α_1G ($Ca_v3.1$) [11], α_1H ($Ca_v3.2$) [12] and α_1I ($Ca_v3.3$) [13]; however, only α_1G and α_1H have been found in pancreatic β-cells [7, 14-21].

T-type Ca^{2+} channel-mediated window current has been recorded in numerous cell types including skeletal muscle fibers, cardiomyocytes, major pelvic ganglion neurons, myoblasts, thalamocortical neurons, and α_1G transfected HEK-293 cells [22-27] and is thought to be a key component in the generation of the slow (<1 Hz) sleep rhythm [28]. There is also evidence that T-type Ca^{2+} channel mediated window current can modulate $[Ca^{2+}]_i$. Chemin *et al*. (2000) demonstrated that varying the concentration of external calcium induced significant changes in $[Ca^{2+}]_i$ in HEK-293 cells over-expressing α_1G [27].

It has been reported that high glucose treatment down regulated high voltage activated Ca^{2+} channels on the plasma membrane both chronically [29, 30] and transiently [31]. However, there has been little data published on the role that elevated glucose plays in regulating T-type Ca^{2+} channel mediated $[Ca^{2+}]_i$ in β-cells. To that end, we hypothesized that antagonism of T-type Ca^{2+} channels either by the selective T-type Ca^{2+} channel antagonist NNC 55-0396 [32] or small interfering RNA (siRNA) will prevent elevations in basal $[Ca^{2+}]_i$ induced by chronically elevated glucose. We proposed that the T-type Ca^{2+} current mediated elevation of basal $[Ca^{2+}]_i$ in β-cells promoted basal insulin release.

MATERIALS AND METHODS

Pancreatic islets isolation and cell culture

Sprague-Dawley rats (Charles River Laboratory, Wilmington, MA, USA) were anesthetized with sodium pentobarbital (1 mg/kg). The pancreas was isolated and the islet cells were collected by the method described previously [29]. Cells were transferred into 35 mm culture dishes and cultured in RPMI 1640 medium (Life Technologies, Rockville, MD, USA) containing 3.3 or 11.1 mM glucose, 10% fetal bovine serum (FBS), 100 U/ml penicillin, and 100 mg/ml streptomycin (P/S) at 37 ^oC, in a humidified atmosphere of 5% CO_2 for 2-5 days before experiments. For experiments requiring unmixed β-cells preparations, β-cells were identified by morphology and by a change in $[Ca^{2+}]_i$ in response to 11.1 mM glucose by Fura-2 fluorescence.

Rat insulinoma cells (INS-1) were cultured in RPMI 1640 medium containing 10% FBS, P/S and 50 μM 2-mercaptoethanol [33] in a humidified atmosphere of 5% CO_2, at 37 ^oC.

siRNA constructs

siRNA constructs were designed against a common motif of α_1G and α_1H using siRNA wizard version 2.4 (Invitrogen, San Diego, CA, USA). The sense sequence was 5'-UGUGA-UGACCUGGAAGAUGGC-3'. Favorable siRNA constructs were obtained from Intergraded DNA Technologies (Coralville, IA, USA). Transfection of siRNA was performed in INS-1 or pancreatic islet cells with Lipofectamine 2000 (Invitrogen) according to the manufacturer's instructions. Briefly, the cells were seeded to ~70% confluency in a 24 well or 35 mm culture dish with a glass cover slip (Fisher, Pittsburg, PA, USA) 24 h before transfection. The next day, siRNA was diluted to 90 pM in a transfection solution (OPTI-MEM I, Gibco, Carlsbad, CA, USA). After 24 h, media was changed to RPMI 1640, 10% FBS and P/S for 48 h. RNA was then harvested with a Trizol Method (Life Technologies) according to the manufacturer's instructions.

Western blot analysis

For analysis of T-type Ca^{2+} channel expression, identical amounts (50 μg) of membrane fraction protein from islet cell lysate were loaded to 7% SDS-PAGE. After transfer to nitrocellulose membranes, the membranes were blocked with 5% skim milk and blotted with primary polyclonal antibodies to the α_1G and α_1H cytoplasmic N-terminus (Alomone Labs, Israel) at 1.5 mg/ml. Following incubation with a goat anti-rabbit secondary antibody (Horseradish Peroxidase), the blots were washed and developed using enhanced

chemiluminescence (ECL, Amersham, Piscataway, NY, USA). Relative intensities of the bands were determined by a GS-700 densitometer (Bio-Rad Laboratories).

Patch clamp electrophysiology

Recordings were carried out using giga-seal whole cell patch methods. Pipette resistance was 2-5 MΩ in intracellular solutions. An EPC-9 patch-clamp amplifier (HEKA, Gottingen, Germany) filtered at 2.9 kHz was used and data was acquired using Pulse/PulseFit software (HEKA). Voltage-dependent currents were corrected for linear leak and residual capacitance by using an on-line P/n subtraction. T-type Ca^{2+} currents were recorded at voltage stepped from -70 to 40 mV in 10 mV increment with a holding potential of -70 mV. Extracellular solutions contained (in mM): 10 $CaCl_2$, 110 tetraethylammonium-Cl (TEA-Cl), 10 CsCl, 10 N-2 hydroxyethylpiperazine-N'-2-ethanesulfonic acid (HEPES), 40 sucrose and 0.5 3, 4-diaminopyridine, at pH 7.3. Intracellular pipette solutions contained (in mM): 130 N-methyl-D-glucamine (NMDG), 10 ethylene glycol tetraacetic acid (EGTA), 15 HEPES, 2 $MgCl_2$, 10 CsCl, 5 NaCl and 1.2 $CaCl_2$ at pH 7.4. After incubation, the β-cells underwent perforated patch clamp electrophysiology. For dual patch clamp and Fura-2 calcium imaging, intracellular solution contained (in mM): 2 $MgCl_2$, 20 sucrose, 10 HEPES, 30 CsCl, 44 CsMs, and 65 CsOH including an additional 50 μM Fura-2 and 175 μM nystatin at pH 7.4 with methanesulfonic acid (MSA).

Calcium imaging

Freshly isolated β-cells or INS-1 cells were plated onto 25 mm glass cover slips. Measurement solution contained (in mM): 125 NaCl, 5.9 KCl, 1.28 $CaCl_2$, 1.2 $MgCl_2$, 17 HEPES and 3.3 glucose, with pH adjusted to 7.4 with NaOH. Cells were incubated with Fura-2 AM for 30 minutes (37 ^oC in 5% CO_2 in a humidified atmosphere) in a loading solution that contained the measurement solution plus 3 μM Fura-2 AM and 3 μL of a 10% pluronic acid solution. Following Fura-2 loading, cells were washed twice and incubated in a Fura-free measurement solution for an additional 20 minutes. Then basal $[Ca^{2+}]_i$ was assessed using measurement solution containing 3.3 glucose or 11.1 mM glucose. Experiments were carried out using an inverted microscope with a 175W Xenon arc lamp Metafluor Imaging System (Nikon Instrument, Lewisville, TX, USA). Data were acquired using MetaFlour 5.0R3 on a P4 1400 MHz processor with 1GB RAM using Windows 2000 Professional SP4.

Quantitative real time PCR

Total RNA was prepared from INS-1 or pancreatic islet cells by using Trizol reagent according to manufacturer's instructions. Real-time quantitative RT-PCR with SYBR® Green detection was performed using GenAmp® PCR system 9600 and GeneAmp® Sequence Detection System version 1.3. Primers were designed using ABI Primer Express™ 2.0. Total RNA was treated with a DNAse (Promega, Madison, WI, USA) prior to cDNA production using a High Capacity cDNA Kit (Invitrogen). Reaction conditions for cDNA synthesis were 80 ºC for 3 minutes and 37 ºC for 2 h.

Each PCR reaction used 100 ng total RNA with the SYBR Green PCR Master Mix (Invitrogen) with 26 μL reaction volumes. The reaction conditions for PCR were (Stage 1, Rep 1x) 50 ºC for 2 minutes, (Stage 2, Rep 1x) 95 ºC for 10 minutes, and (Stage 3, Rep 40x) 95 ºC for 15 seconds and then 60 ºC for 1 minute.

Insulin secretion analysis

Isolated rat islet cells were plated on 35 mm culture dishes and incubated in 3.3 mM glucose medium for 3 days or treated with siRNA 6 h after plating. Before undergoing ELISA, cells were washed with Hank's Balanced Salt Solution (HBSS) containing 3.3 mM glucose 3x. Groups were then treated with HBSS with 3.3 mM glucose (control and siRNA treated) or 3.3 mM glucose plus 8 μM NNC 55-0396 for 90 minutes. Then 10 μL of the solution was aspirated and placed on ice before being subjected to a High Range Insulin ELISA (ALPCO Windham, NH, USA) according to manufacturer's instructions.

Animal studies

Obese homozygote (db^-/db^-) type 2 diabetic mice lacking the gene encoding for leptin receptor (diabetic, 8-10 weeks old) and heterozygote leptin

receptor (db^-/db^+) nondiabetic (control, 8-10 weeks old) adult male mice were obtained from The Jackson Laboratories (Bar Harbor, MA, USA). Ca^{2+} channel blockers (mibefradil, NNC 55-0396 and nicardipine) were injected 30 mg/kg/day (i.p.). Blood glucose measurements were obtained from tail blood samples using a blood glucose meter (Prestige Smart System HDI; Home Diagnostic, Ft. Lauderdale, FL, USA) in all groups after 6 h of fasting. Steady-state insulin level was determined by using the Mercodia Ultrasensitive Mouse Insulin ELISA protocol (enzyme immunoassay), according to the manufacturer's recommendations.

Statistical analysis

All data were reported as mean ± SEM, statistical significance was determined using $p < 0.05$ with a Student's two-tailed t-test or a one-way ANOVA. Statistical analysis was performed with Graphpad Prism 4.0.

RESULTS

Chronic incubation of 11.1 mM glucose resulted in an increased T-type Ca^{2+} channel current in rat islet cells. Figure 1A and 1B compares two representative family Ca^{2+} current traces recorded from cells incubated in 3.3 mM or 11.1 mM glucose for 48 h, respectively. In the high glucose treated cells, fast inactivated currents were recorded at voltages between -30 to 0 mV, representing a typical characterization of T-type Ca^{2+} channel currents. In contrast, the Ca^{2+} currents recorded in the 3.3 mM glucose treated cell shows mainly sustained currents, which represent the characterization of non-T-type Ca^{2+} currents. A plot of I-V relationship from accumulated measurements shows that the peaks of Ca^{2+} currents in 11.1 mM glucose treated cells are at 20 to 30 mV more negative than that of 3.3 mM glucose treated cells (Figure 1C).

In order to further explore the molecular mechanism of high glucose induced up-regulation of T-type Ca^{2+} channels, we examined the mRNA of T-type Ca^{2+} channels in freshly isolated rat islets in either 3.3 or 11.1 mM glucose over a 48 h time period. Quantitative real time PCR was used to determine the mRNA levels of α_1G and α_1H. Figure 1D shows that the relative message expression for α_1G (1A) increased 3.1X and 3.3X after 24 and 48 h, respectively, when incubated in 11.1 mM glucose. Similarly, α_1H (Figure 1E) message expression increased 1.4X and 1.8X after 24 and 48 h, respectively, when incubated under similar conditions. Expression of α_1G and α_1H did not change up to 48 h incubation in 3.3 mM glucose. Protein expression of T-type Ca^{2+} channels also increased after incubation in 11.1 mM glucose for 72 h (Figure 1F).

Next we suspected that T-type Ca^{2+} channel current might exhibit a sustained inward Ca^{2+} window current at voltages near the threshold of the channel activation. To prove the principle, we chose to use a pancreatic β-cell line, INS-1, which has a higher level of T-type Ca^{2+} channel currents, to elaborate the properties of T-type Ca^{2+} channel window currents. Figure 2A shows several traces of Ca^{2+} currents recorded at low voltages from an INS-1 cell. A portion of these currents was inactivated during the first 100 ms, whereas the remaining currents (window currents) were activated continuously over 500 ms. Figure 2B shows the sustained current amplitude changes in three representative current tracings elicited at three different test pulses (-64, -52 and -40 mV). The sustained current amplitudes measured in the hatched box position are plotted as a bell shaped curve (Figure 2C), which characterizes peak T-type Ca^{2+} channel mediated window current in our experimental voltage protocol; the increase in the sustained current in Figure 2C greater than -40 mV can be attributed to the activation of L-type Ca^{2+} channels. Figure 2D shows a representative 2 second sustained window current trace of approximately 10 pA from a rat islet cell (holding potential -80 mV, test pulse -55 mV). The current/voltage (I/V) relationship of this window current is plotted in Figure 2E. Next, we examined whether a window current would result in changes in intracellular calcium by employing the dual patch clamp electrophysiology and Fura-2 calcium imaging technique to measure the change of intracellular Ca^{2+} concentration corresponding to the small membrane depolarization. Figure 2F represents changes in $[Ca^{2+}]_i$ from an islet cell in response to a low voltage elicited window current (holding potential -80 mV, test pulse -55 mV, 100 seconds).

If T-type Ca^{2+} channel window current mediated Ca^{2+} entry occurred under the non-stimulus

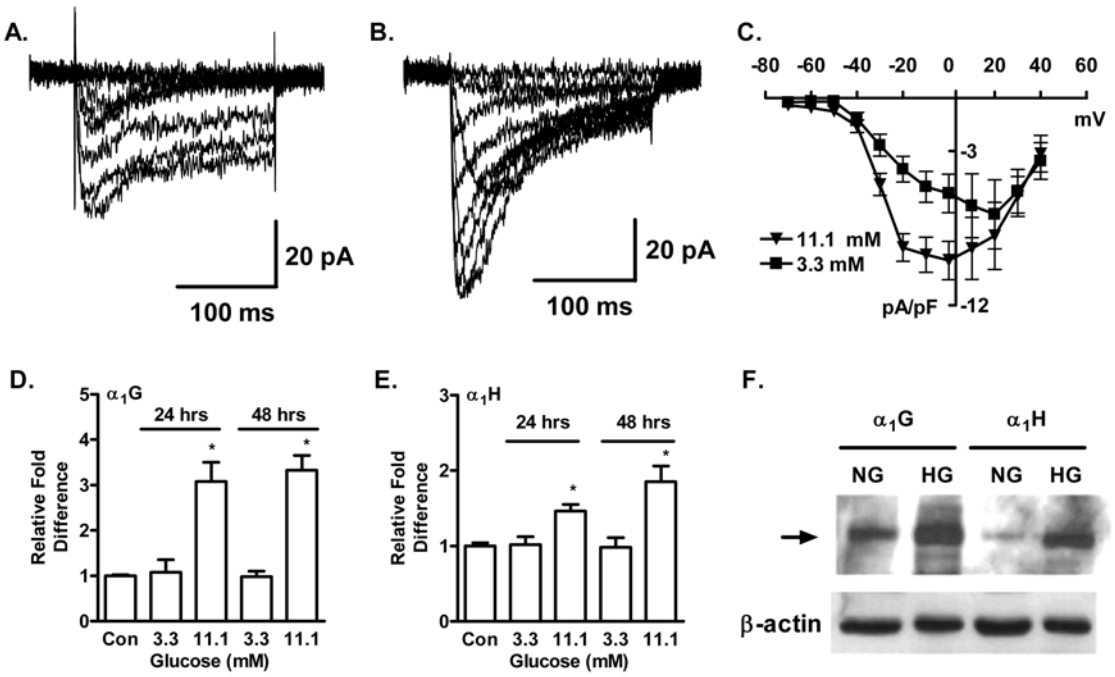

Figure 1. A and B: representative T-type Ca^{2+} channel current families elicited from isolated rat islet cells at variable voltages after a 48 h treatment with either 3.3 or 11.1 mM glucose, respectively. C: averaged current-voltage relationship under A and B conditions, n = 6. D and E: isolated rat islet cells were treated with either 3.3 or 11.1 mM glucose and for either 24 or 48 h and the α_1G and α_1H expression levels were examined with quantitative real time PCR. Control expression levels were from freshly isolated rat islets, n = 3, *p < 0.01. Sequences for RT-PCR primers were as follows: α_1H forward 5'-TCCCCAACTTTGCCTTTGAC-3' and reverse 5'-TGGTCACTGTCCAAGAAACAGTCT-3' calibrator was β-actin forward 5'-ACGAGGCCCAGAGCAAGA-3' and reverse 5'-GTTGGTTACAATGCCGTGTTCA-3'. For α_1G, the sequences were forward 5'-TCCCAGCAGCCA GGAAGA-3' and reverse 5'-CTGGGTCTCTACACTGTAGCACTTCT-3' calibrator was β-actin forward 5'-CTT CAACACCCCAGCCATGT-3' and reverse 5'-GTGGTACGACCAGAGGCATACA-3'. F: Western blot analysis show increased α_1G and α_1H protein expression in rat islet cells after 11.1 mM glucose incubation for 72 h. NG: normal glucose (3.3 mM). HG: high glucose (11.1 mM).

(no action potentials) conditions, one would expect that increased T-type Ca^{2+} channel expression resulting from chronic high glucose incubation would increase basal intracellular Ca^{2+} concentration. To test this idea, Fura-2 fluorescence imaging was employed to measure the basal Ca^{2+} concentration in islet cells that had been cultured in different glucose concentrations for 48 h. Figure 3A shows that islet cells incubated in 11.1 mM glucose had significantly elevated intracellular calcium (192 ± 8.0 nM) compared to controls (72.3 ± 4.6 nM).

In order to learn the physiological function of T-type Ca^{2+} channels in regulating basal Ca^{2+} concentration in islet cells, we next tested if blockage of T-type Ca^{2+} channels would reduce basal $[Ca^{2+}]_i$ in isolated β-cells cultured in normal glucose (3.3 mM). Using Fura-2 calcium imaging, $[Ca^{2+}]_i$ was measured before and after treatment with 8 μM NNC 55-0396. As shown in Figure 3B, averaged $[Ca^{2+}]_i$ from 9 experiments decreased as NNC 55-0396 was perfused into the recording chamber. Washing out NNC 55-0396 did not significantly elevate $[Ca^{2+}]_i$, however, we previously reported [32] that NNC 55-0396 is resistant to this phenomena.

In addition to using a channel antagonist to inhibit window current, we used siRNA to further verify the role that α_iG and α_iH play in the elevation of $[Ca^{2+}]_i$ in β-cells. Figure 4A and 4B shows that cells treated with the siRNA against both α_iG and α_iH subunits of T-type Ca^{2+} channels for 72 h

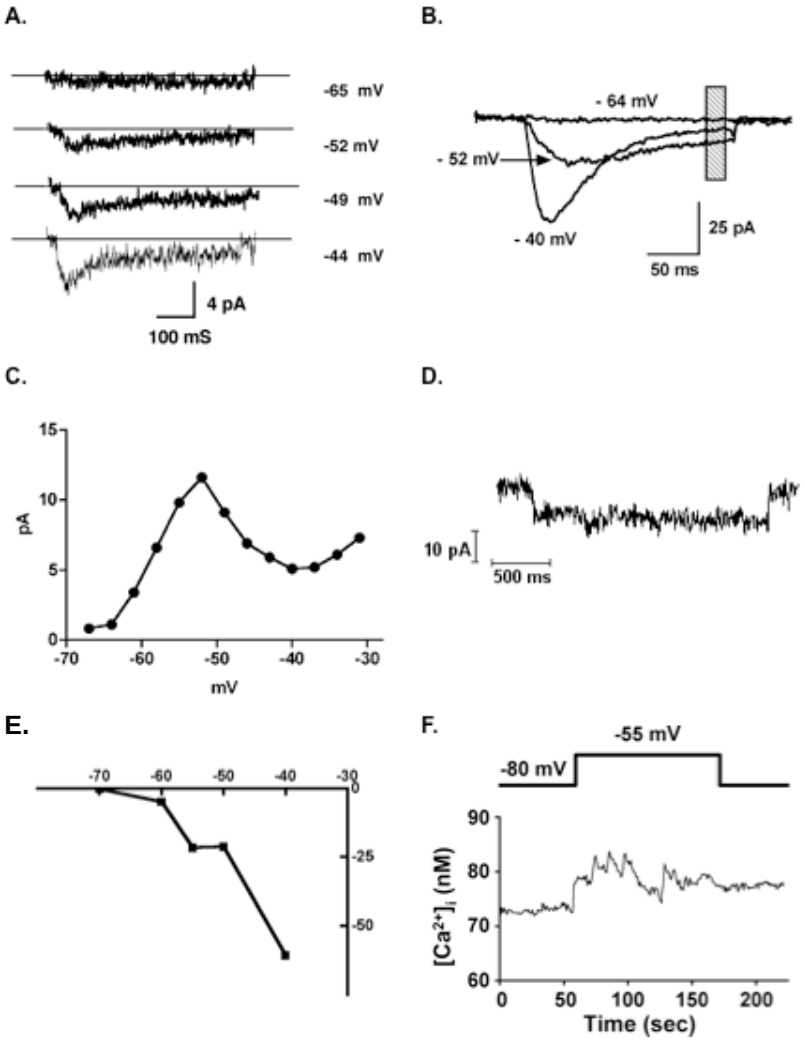

Figure 2. A: long lasting Ca^{2+} currents recorded at low voltage in rat islet cells. B: current tracings from INS-1 cells, sustained inward current in hatched area are plotted in C. C: I/V plot of hatched area recorded in B. D: dual patch clamp/Fura-2 fluorescence measurement, current elicited from same rat β-cell at -55 mV, a sustained inward current can be observed. E: I/V plot of the current observed during the window current pulse. F: rise in rat β-cell $[Ca^{2+}]_i$ in response to a change in membrane potential at -55 mV. Emitting fluorescent signal (510 nM) was acquired by an ADC 20 MHz camera (Photometric Coolsnap FX Monochrome, Nikon). Acquisition time was 250 ms and the empirical K_d obtained for Ca^{2+} binding to Fura-2 was 269 nM.

have decreased expression of α_1G and α_1H (75% and 77% decrease, respectively). In contrast, scrambled siRNA did not result in a change in expression (Figures 4A and 4B). Transfection efficiency was tested using siRNA tagged with fluorescein. Confocal microscopy showed a greater than 90% transfection in both INS-1 and rat β-cells (data not shown). To confirm the reduction of mRNA by siRNA translating into a reduction in T-type Ca^{2+} channel current, patch clamp electrophysiology was used at 72 h post siRNA transfection. Figure 4C shows representative traces recorded from INS-1 cells that were treated or untreated (control) with siRNA against both α_1G and α_1H subunits of T-type Ca^{2+} channels. Figure 4D shows the siRNA caused an 80% reduction in T-type Ca^{2+} channel currents measured at -20 mV versus that from the untreated cells.

To verify the role of T-type Ca^{2+} channels in modulating β-cell basal $[Ca^{2+}]_i$ in response to

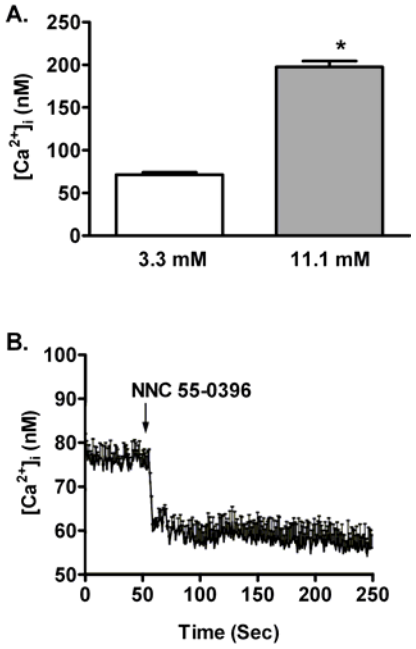

Figure 3. A: isolated rat islet cells treated with 3.3 or 11.1 mM glucose for 48 h. $[Ca^{2+}]_i$ measured by Fura-2 fluorescence, n = 18, *p < 0.01. B: averaged $[Ca^{2+}]_i$ tracing of β-cells measured by Fura-2 fluorescence. Eight μM NNC 55-0396 was perfused at arrow mark, n = 9.

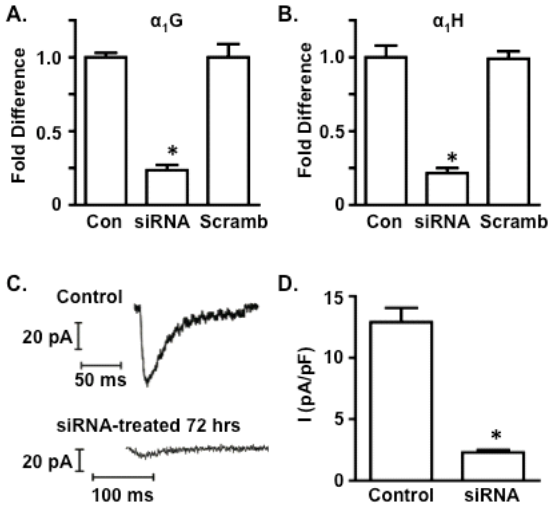

Figure 4. A and B: effect of siRNA on α_1G and α_1H mRNA levels in islet cells. Quantitative RT-PCR examined mRNA levels 72 h post transfection, n = 11. C: patch clamp recording of islet cells treated and untreated (control) with siRNA for 72 h. D: averaged amplitude of peak T-type Ca^{2+} channel currents measured at -20 mV in islet cells in control (left) or siRNA treated cells (right), n = 6, *p < 0.01.

elevated glucose, we incubated rat islet cells in 11.1 mM glucose for 72 h with siRNA. Figure 5A shows a significant decrease in $[Ca^{2+}]_i$ in rat islet cells treated with the siRNA targeting T-type Ca^{2+} channels, but not in cells treated with the scrambled siRNA.

It is commonly known that changes in $[Ca^{2+}]_i$ are vital for stimulus induced insulin secretion. However, little is known about the role of basal calcium on basal insulin release. Since T-type Ca^{2+} channels play a significant role in basal calcium levels, we investigated the relationship between basal calcium and basal insulin release. Figure 5B shows basal insulin levels from rat islet cells incubated in 3.3 mM glucose and treated with siRNA or NNC 55-0396 versus controls. The data show that cells treated with the siRNA had significantly decreased basal insulin release. Similarly, cells treated with 8 μM NNC 55-0396 had significantly decreased basal insulin release over a 90 minute period (Figure 5C). The scrambled siRNA did not significantly lower the basal insulin secretion.

To directly link basal intracellular Ca^{2+} concentration with basal insulin release, we used a cell permeable calcium chelator nitrophenyl-EGTA (NP-EGTA) to examine insulin release over a 90 minute period. Figure 5D shows that chelation of intracellular calcium resulted in significantly (25%) decreased basal insulin secretion.

It was interesting to learn whether the blockade of T-type Ca^{2+} channels *in vivo* would have an effect on the basal insulin level. To conduct this experiment, we chose to test a T-type Ca^{2+} channel blocker mibefradil on basal level of insulin in db^-/db^- diabetic mice and db^+/db^- non-diabetic mice. We used mibefradil instead of NNC-55-0396 since the pharmacological mechanism of this agent is better characterized *in vivo*. As shown in Figure 6A, mibefradil (30 mg/kg/day, i.p.) reduced basal insulin from 5.09 ± 0.23 to 3.18 ± 0.05 ng/mL ($p < 0.01$) in diabetic mice. In contrast, no significant reduction of basal insulin in non-diabetic mice was observed.

Interestingly, mibefradil also effectively reduced fasting glucose level in db^-/db^- diabetic mice as shown in Figure 6B. Average glucose level of

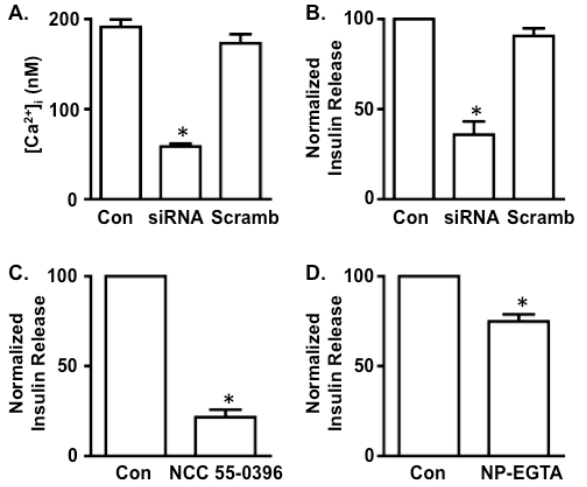

Figure 5. A: rat islet cells treated with 11.1 mM glucose (control), siRNA, or scrambled siRNA for 72 h. $[Ca^{2+}]_i$ measured by Fura-2 fluorescence, n = 8-11, *p < 0.01. B: siRNA effect on basal insulin secretion on rat β-cells. Insulin secretion was examined with ELISA under 3 mM glucose for 90 minutes after 72 h siRNA treatment, scrambled siRNA treatment, or control, n = 7. C: NNC 55-0396 effect on basal insulin secretion on rat β-cells. Insulin secretion was examined under 3 mM glucose for 90 minutes with and without 8 μM NNC 55-0396, n = 4, *p < 0.01. D: NP-EGTA effect on basal insulin secretion on rat β-cells. NP-EGTA was incubated for 20 minutes, then washed twice and incubated in a NP-EGTA-free measurement solution for an additional 20 minutes. Basal insulin secretion was examined with ELISA under 3 mM glucose for 90 minutes after NP-EGTA treatment or control, n = 4, *p < 0.01.

db^-/db^- mice was reduced from 352 ± 47.16 mg/mL to 136 ± 52.12 in 24 h after mibefradil treatment (30 mg/kg/day, i.p.). This reduced fasting glucose remains at similar level for the entire experimental period of 10 days. The fasting glucose level of db^-/db^- mice without the mibefradil treatment stayed at ~390 mg/mL level throughout the experimental period. Mibefradil showed a much smaller effect on reduction of the fasting glucose in the heterozygote db^-/db^+ nondiabetic mice. To further characterize the pharmacological effect of mibefradil on fasting glucose level in db^-/db^- mice, we tested the effects of other Ca^{2+} channel blockers on the fasting glucose level in these animals. The fasting glucose levels of mice at the 72 h are shown in Figure 6C. T-type Ca^{2+} channel blocker NNC 55-0396 had a similar effect as mibefradil: lowering fasting glucose level of db^-/db^- mice dramatically. In contrast, L-type Ca^{2+} channel blocker nicardipine had no effect on the fasting glucose level in the db^-/db^- mice. No significant effect of mibefradil, NNC 55-0396 or nicardipine on the fasting glucose levels was observed in the control animals. Therefore, the hypoglycemic effect of these Ca^{2+} channel blockers may attribute their antagonism to the T-type Ca^{2+} channels rather than to the L-type Ca^{2+} channels.

DISCUSSION

Our study targets directly on the cause of hyperinsulinemia in the prediabetic condition.

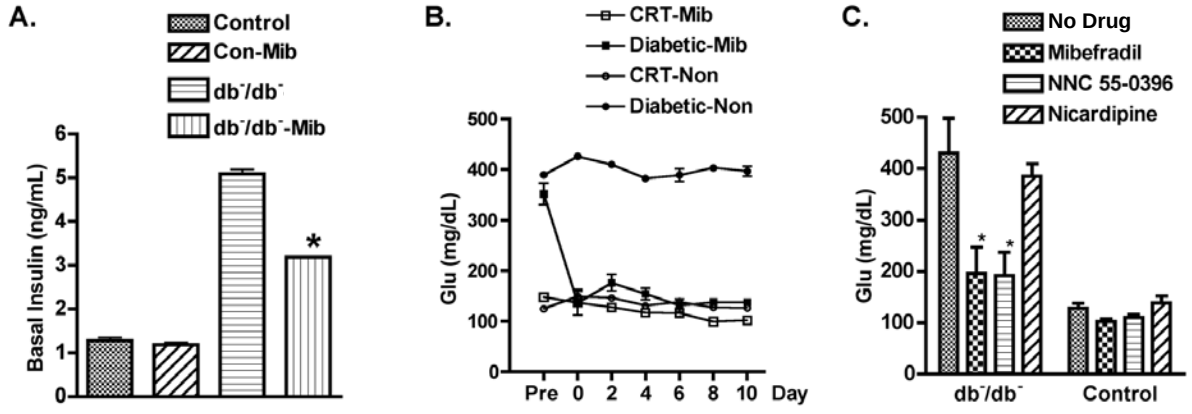

Figure 6. A: basal insulin levels measured in mibefradil treated and non-treated $lepr^{db-/db-}$ diabetic mice (n = 5) and control $lepr^{db+/db-}$ mice (n = 6). *p < 0.01 when compared with non-treated diabetic mice. B: fasting glucose measured after mibefradil injection in $lepr^{db-/db-}$ diabetic mice and controls, n = 5. C: effect of calcium channel blockers on the fasting glucose in $lepr^{db-/db-}$ diabetic mice and controls, n = 6. Mib: mibefradil; db^-/db^-: $lepr^{db-/db-}$; Control: $lepr^{db+/db-}$. *p < 0.01 when compared with non-treated diabetic mice.

We propose that fluctuation of high plasma glucose concentration and other associate factors (inflammatory cytokines [10], genetic predisposition, etc.) causes increased pancreatic β-cells T-type Ca^{2+} channel expression, which in turn, leads to elevation of basal $[Ca^{2+}]_i$ and chronic basal insulin release.

A major finding of this study was that an increase in extracellular glucose could promote the transcription and increase the current of T-type Ca^{2+} channels in pancreatic islet cells. While the mechanism behind this effect on these channels remains elusive, this study presents direct evidence to support the hypothesis that chronically elevated glucose contributes significantly to increased T-type Ca^{2+} channel mRNA level and depolarization induced current. These results are not seen in high voltage activated Ca^{2+} channels (α_1B, α_1C, α_1D) which were decreased by chronic high glucose treatments [29].

T-type Ca^{2+} channel mediated window current was found in both INS-1 and rat pancreatic islet cells and was correlated with increased $[Ca^{2+}]_i$ using a well established dual patch clamp/calcium imaging technique (Figure 2). Interestingly, the rise in $[Ca^{2+}]_i$ remained elevated even after cells were brought back to the holding potential. It is possible that the small increase in intracellular calcium may not adequately activate calcium homeostatic machinery.

Another important finding in the present study was that T-type Ca^{2+} channels and basal calcium have a direct effect on basal insulin release in rat islets. Application of the T-type Ca^{2+} channel antagonist NNC 55-0396 or T-type Ca^{2+} channel specific siRNA results in decreased basal calcium and decreased basal insulin secretion in the islet cells or islets, similar to the effect of NNC 55-0396 on INS-1 cells reported previously [29]. Furthermore, lowering intracellular calcium using the calcium chelator, NP-EGTA, caused a significant decrease in basal insulin secretion, indicating that elevated basal $[Ca^{2+}]_i$ is a determining factor of increased insulin release in pancreatic β-cells and thus may play a central role in low threshold exocytosis [34].

T-type Ca^{2+} channel blocker NNC 55-0396 has been shown to inhibit low glucose (6 mmol/l) induced insulin release in human pancreatic β-cells [35]. Here we show that mibefradil reduces basal insulin level in the diabetic animals. This supports the notion that T-type Ca^{2+} channels play an important function in basal insulin release of diabetic animals.

The hypoglycemic effect of mibefradil and NNC 55-0396 took place quickly, therefore it may not directly relate to the reduction of basal insulin level in these animals. However, it is clear that mibefradil's hypoglycemic effect was not due to its inhibition of L-type Ca^{2+} channels [36], because the L-type Ca^{2+} channel blocker nicardipine did not have the hypoglycemic effect (Figure 6). It is especially interesting to know how the hypoglycemic effect relates to T-type Ca^{2+} channel function in the db^-/db^- diabetic animals.

In conclusion, we have shown that T-type Ca^{2+} channels play an important part in regulating basal $[Ca^{2+}]_i$, which was then associated with alterations in basal insulin secretion.

CONFLICT OF INTEREST STATEMENT

The authors have no conflict of interest to disclose.

REFERENCES

1. Warram, J. H., Martin, B. C., Krolewski, A. S., Soeldner, J. S. and Kahn, C. R. 1990, Ann. Intern. Med., 113, 909.
2. Haffner, S. M., Stern, M. P., Dunn, J., Mobley, M., Blackwell, J. and Bergman, R. N. 1990, Metabol., 39, 842.
3. Hellman, B., Berne, C., Grapengiesser, E., Grill, V., Gylfe, E. and Lund, P. E. 1990, Eur. J. Clin. Invest., 20, S10.
4. Levy, J., Gavin, J. R. 3rd and Sowers, J. R. 1994, Am. J. Med., 96, 260.
5. Bjorklund, A., Lansner, A. and Grill, V. E. 2000, Diabetes, 49, 1840.
6. Kahn, S. E., Klaff, L. J., Schwartz, M. W., Beard, J. C., Bergman, R. N., Taborsky, G. J. Jr. and Porte, D. Jr. 1990, J. Clin. Endocrinol. Metab., 71, 994.
7. Bokvist, K., Eliasson, L., Ammala, C., Renstrom, E. and Rorsman, P. 1995, EMBO J., 14, 50.
8. Barg, S., Ma, X., Eliasson, L., Galvanovskis, J., Göpel, S. O., Obermüller, S., Platzer, J.,

Renström, E., Trus, M., Atlas, D., Striessnig, J. and Rorsman, P. 2001, Biophys. J., 81, 3308.
9. Misler, S., Barnett, D. W., Gillis, K. D. and Pressel, D. M. 1992, Diabetes, 41, 1221.
10. Wang, L., Bhattacharjee, A., Fu, J. and Li, M. 1996, Diabetes, 45, 1678.
11. Perez-Reyes, E., Cribbs, L. L., Daud, A., Lacerda, A. E., Barclay, J., Williamson, M. P., Fox, M., Rees, M. and Lee, J. H. 1998, Nature, 391, 896.
12. Cribbs, L. L., Lee, J. H., Yang, J., Satin, J., Zhang, Y., Daud, A., Barclay, J., Williamson, M. P., Fox, M., Rees, M. and Perez-Reyes, E. 1998, Circ. Res., 83, 103.
13. Lee, J. H., Daud, A. N., Cribbs, L. L., Lacerda, A. E., Pereverzev, A., Klöckner, U., Schneider, T. and Perez-Reyes, E. 1999, J. Neurosci., 19, 1912.
14. Davalli, A. M., Biancardi, E., Pollo, A., Socci, C., Pontiroli, A. E., Pozza, G., Clementi, F., Sher, E. and Carbone, E. 1996, J. Endocrinol., 150, 195.
15. Velasco, J. M., Petersen, J. U. and Petersen, O. H. 1988, FEBS Lett., 231, 366.
16. Hiriart, M. and Matteson, D. R. 1988, J. Gen. Physiol., 91, 617.
17. Bhattacharjee, A., Whitehurst, R. M. Jr., Zhang, M., Wang, L. and Li, M. 1997, Endocrinol., 138, 3735.
18. Iwashima, Y., Pugh, W., Depaoli, A. M., Takeda, J., Seino, S., Bell, G. I. and Polonsky, K. S. 1993, Diabetes, 42, 948.
19. Zhuang, H., Bhattacharjee, A., Hu, F., Zhang, M., Gosmami, T., Wang, L., Wu, S., Berggren, P.-O. and Li, M. 2000, Diabetes, 49, 59.
20. Navarro-Tableros, V., Fiordelisio, T., Hernandez-Cruz, A. and Hiriart, M. 2007, Am. J. Physiol., 292, E1018.
21. Yang, S. N. and Berggren, P. O. 2006, Endocr. Rev., 27, 621.
22. Hughes, S. W., Cope, D. W., Toth, T. I., Williams, S. R. and Crunelli, V. 1999, J. Physiol., 517, 805.
23. Leuranguer, V., Monteil, A., Bourinet, E., Dayanithi, G. and Nargeot, J. 2000, Am. J. Physiol., 279, H2540.
24. Lee, J. H., Kim, E. G., Park, B. G., Kim, K. H., Cha, S. K., Kong, I. D., Lee, J. W. and Jeong, S. W. 2002, J. Neurophysiol., 87, 2844.
25. Bijlenga, P., Liu, J. H., Espinos, E., Haenggeli, C. A., Fischer-Lougheed, J., Bader, C. R. and Bernheim, L. 2000, Proc. Natl. Acad. Sci. USA, 97, 7627.
26. Berthier, C., Monteil, A., Lory, P. and Strube, C. 2002, J. Physiol., 539, 681.
27. Chemin, J., Monteil, A., Briquaire, C., Richard, S., Perez-Reyes, E., Nargeot, J. and Lory, P. 2000, FEBS Lett., 478, 166.
28. Hughes, S. W., Cope, D. W., Blethyn, K. L. and Crunelli, V. 2002, Neuron, 33, 947.
29. Taylor, J. T., Huang, L., Keyser, B. M., Zhuang, H., Clarkson, C. W. and Li, M. 2005, Am. J. Physiol., 289, E900.
30. Kato, S., Ishida, H., Tsuura, Y., Tsuji, K., Nishimura, M., Horie, M., Taminato, T., Ikehara, S., Odaka, H., Ikeda, I., Okada, Y. and Seino, Y. 1996, J. Clin. Invest., 97, 2417.
31. Huang, L., Bhattacharjee, A., Taylor, J. T., Zhang, M., Keyser, B. M., Marrero, L. and Li, M. 2004, Am. J. Physiol., 286, C213.
32. Huang, L., Keyser, B. M., Tagmose, T. M., Hansen, J. B., Taylor, J. T., Zhuang, H., Zhang, M., Ragsdale, D. S. and Li, M. 2004, J. Pharmacol. Exp. Ther., 309, 193.
33. Asfari, M., Janjic, D., Meda, P., Li, G., Halban, P. A. and Wollheim, C. B. 1992, Endocrinol., 130, 167.
34. Weiss, N., Hameed, S., Fernández-Fernández, J. M., Fablet, K., Karmazinova, M., Poillot, C., Proft, J., Chen, L., Bidaud, I., Monteil, A., Huc-Brandt, S., Lacinova, L., Lory, P., Zamponi, G. W. and De Waard, M. 2012, J. Biol. Chem., 287, 2810.
35. Braun, M., Ramracheya, R., Bengtsson, M., Zhang, Q., Karanauskaite, J., Partridge, C., Johnson, P. R. and Rorsman, P. 2008, Diabetes, 57, 1618.
36. Moosmang, S., Haider, N., Bruderl, B., Welling, A. and Hofmann, F. 2006, Circ. Res., 98, 105.